Aerodynamic Design of the 13.2 MW SUMR-13i Wind Turbine Rotor

Gavin K. Ananda,[*] Suraj Bansal,[†] and Michael S. Selig[‡]
University of Illinois at Urbana–Champaign, Urbana, IL 61801, USA

In an effort to precipitate the development of US wind energy capabilities, the Advanced Research Projects Agency for Energy (ARPA-E, US Department of Energy) funded a project to ultimately design a low-cost 50 MW offshore wind turbine rotor. To achieve the aim of designing a new, low-cost, extreme-scale wind turbine, the Segmented Ultralight Morphing Rotor (SUMR) concept was proposed to reduce the rotor mass and consequently, the levelized cost of energy when compared to conventional design methods. The SUMR concept involves morphing a downwind rotor such that the mean blade loads are closely aligned with the blade axis, thus reducing the bending loads and allowing for a lighter blade design. The SUMR concept is being initially implemented on a smaller-scale 13.2 MW wind turbine and will be subsequently applied on the larger-scale 50 MW size. This paper elaborates the detailed aerodynamic design of the downwind, two-bladed, offshore, horizontal-axis, 13.2 MW SUMR-13i (initial) wind turbine rotor. The paper begins by introducing the system-level considerations that influence the aerodynamic design requirements, followed by a discussion of the actual design process. The tools for the aerodynamic design of the airfoils and blades are presented next, following which different design iterations have been described. A new family of flatback airfoils, the F1-family, with maximum thicknesses varying from 17–48% and capable of operating in the Reynolds number range of 4,000,000 to 15,000,000, was designed to be used on the SUMR-13i rotor. The rotor in each design iteration was optimized to operate at the tip speed ratio of 9.5 at a rated speed of 11.3 m/s and a coning angle of 12.5 deg, which resulted in a rotor diameter of 213.7 m. Finally, the performance of the final design has been described in terms C_p vs TSR curves and blade load variation with coning angle.

Nomenclature

a	=	axial induction factor
c	=	chord
C	=	centrifugal force
C_d	=	two-dimensional drag coefficient
C_l	=	two-dimensional lift coefficient
C_p	=	rotor power coefficient
G	=	gravitational force
k	=	turbulent kinetic energy
m	=	mass
N_{crit}	=	critical number in the e^n theory
P	=	power
r	=	radius from the axis of rotation
R	=	rotor tip radius
Re	=	Reynolds number based on chord c ($= V_\infty c/\nu$)
Re_{θ_t}	=	transition momentum-thickness Reynolds number
t	=	thickness of the blade/airfoil
T	=	thrust force
Ti	=	turbulence intensity

[*]Graduate Research Assistant (Ph.D. Candidate), Department of Aerospace Engineering, 104 S. Wright St., AIAA Student Member. anandak1@illinois.edu
[†]Graduate Research Assistant, Department of Aerospace Engineering, 104 S. Wright St., AIAA Student Member. sbansal5@illinois.edu
[‡]Professor, Department of Aerospace Engineering, 104 S. Wright St., AIAA Associate Fellow. m-selig@illinois.edu

TSR	=	tip speed ratio ($=\frac{\Omega R \cos\beta}{V}$)
V	=	wind velocity
α	=	angle of attack
β	=	rotor cone angle
γ	=	intermittency
ν	=	kinematic viscosity
ω	=	specific rate of dissipation of turbulent kinetic energy k
Ω	=	rotational speed of the rotor
ρ	=	density of air

Subscripts

∞	=	freestream conditions
avg	=	corresponding to average wind speed conditions
blade	=	pertaining to the wind turbine blades
cut $-$ out	=	corresponding to the cut-out wind speed conditions
rated	=	corresponding to rated wind speed conditions

I. Introduction

The trend toward the use of large offshore wind turbines in a bid to maximize power production capabilities and reduce the overall cost of energy has necessitated the need to build extreme-scale wind turbines. To meet the aim envisioned by the US Department of Energy (DOE), which is to produce 20 percent of electricity by the year 2030 using wind energy,[1] the Advanced Research Projects Agency – Energy (ARPA-E) arm of DOE recently awarded a contract to a group of institutions§to design a low-cost offshore 50 MW wind turbine in order to help accelerate the development of the US offshore wind energy capability.[2]

Designing such extreme-scale turbines using conventional methods will result in a considerable amount of technical barriers. For instance, at these scales the primary design limitations are imposed due to the large rotor weight and several structural considerations. Longer blades are required to increase power production; however, the large bending loads resulting from the combination of gravitational and aerodynamic loads on the blade at these scales will result in root diameters of extreme sizes for sound structural performance in all wind condition. Some of the other difficulties when designing using conventional method will involve a) enormous rotor mass at such extreme-scales (about 200 m blade length for the 50 MW wind turbine) due to the required high blade stiffness to avoid tower strikes, b) difficulty in building and transporting the rotor blades due to the large blade size, and c) exorbitant cost of energy.[3,4].

The ARPA-E funded SUMR (Segmented Ultralight Morphing Rotor) project intends to address this critical issue and eventually engender the design of low-cost 50 MW wind turbines with potentially 200 m long blades. The SUMR concept involves morphing a downwind rotor similar to swaying and bending of palm trees under high wind loads to reduce root bending moments. The blades can be coned in such a way that the combination of gravitational, centrifugal, and aerodynamic loads acting on the blade are closely aligned along the blade axis. The alignment of these loads along the axis of the blade (see Fig. 1), in essence, allows for the blades to be designed to be drastically thinner and lighter.[5–7] Morphing the rotor blades to such load-aligned configurations will lead to a drastic reduction in the blade mass and consequently result in a lower levelized cost of energy (LCOE).

This paper discusses the methodology for the aerodynamic design of an extreme-scale rotor (13.2 MW) capable of coning up to 12.5 deg at the rated conditions. The study begins by identifying the system level requirements set by other sub-teams within the ARPA-E SUMR team that affect the aerodynamic design of the rotor. For example, a specific thickness for the blade cross-section may be specified near the hub region by the structures team based on bending load considerations. Once these system level requirements have been taken into account, the actual design process will be discussed which outlines the aerodynamic design philosophy followed in this study to maximize the rotor performance. The aerodynamic design and analysis tools readily available to implement the aforementioned

---

§The group of institutions is comprised of: 1) University of Virginia (team lead and morphing group), 2) University of Illinois at Urbana-Champaign (aerodynamics group), 3) University of Colorado-Boulder (controls group), 4) Colorado School of Mines (control group), 5) Sandia National Labs/University of Dallas (structures group), and 6) National Renewable Energy Labs (field testing group).
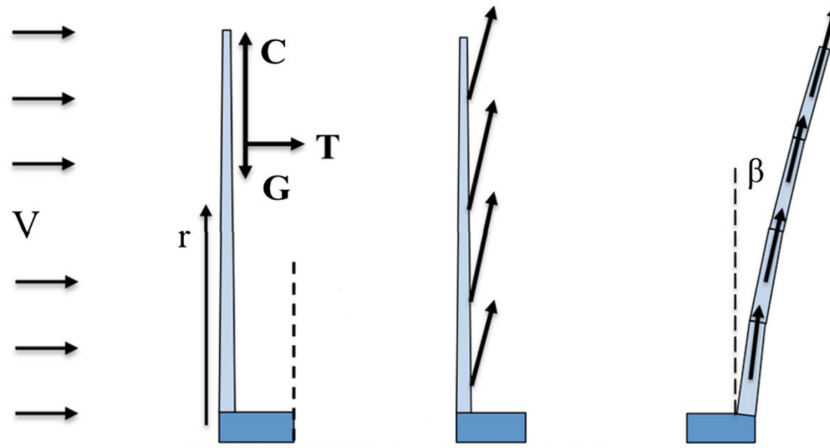
American Institute of Aeronautics and Astronautics

Figure 1. Diagram depicting load alignment for a morphing downwind rotor at rated conditions to reduce cantilever moments. [4]

design philosophy in the actual rotor design will also be discussed. Finally, the manner in which different sub-teams comprising primarily of aerodynamics, structures, and controls interdepend on one another and the way controls and structural considerations affect the aerodynamic design of an extreme-scale morphing rotor will be described in the design iterations section.

II. System Level Requirements

The ultimate goal of the SUMR project is to design a low-cost 50 MW offshore wind turbine. However, the SUMR concept will be initially applied to a smaller scale 13.2 MW SUMR-13i wind turbine rotor (where 'i' in the SUMR-13i stands for 'initial') as a starting point and the mass reduction benefits will be compared to the 13.2 MW conventional three-bladed horizontal axis upwind rotor design (CONR wind turbine) based on the Sandia National Lab's 100 m blade (see Table 1). [8,9] The location of the wind turbine plays an important role in its performance and the levelized cost of energy. Based on numerous considerations, the IEC Class IIB location which is the Dominion Virginia Offshore Lease Zone was selected as the location where the SUMR-13i rotor will be designed to operate. The average and rated speeds at this location based on a 100 m hub height are 8.5 and 11.3 m/s respectively. Key details for the CONR are presented in Table 1. Key details for the SUMR-13i are left empty in Table 1. With the goal of a 25% reduction in rotor mass compared to the CONR, the design process and final design of the SUMR-13i will be discussed in the proceeding sections of this paper.

Table 1. CONR Design Specifications

Metric	CONR	SUMR-13i
Rated Power (P_{rated})	13.2 MW	13.2 MW
Avg. Wind Speed (V_{avg})	8.5 m/s	8.5 m/s
Rated Wind Speed (V_{rated})	11.3 m/s	11.3 m/s
Cut-out Wind Speed ($V_{cut-out}$)	25 m/s	25 m/s
Rotor Radius (R)	102.5 m	-
Rated Rotor Speed (Ω)	7.44 RPM	-
Tip-Speed Ratio (TSR)	9.66	-
Rotor Orientation	Upwind	-
Number of Blades (B)	3	-
Cone Angle (β)	−2.5	-
Blade Mass (m_{blade})	49,519 kg	-
Rotor Mass (m_{rotor})	148,500 kg	-

American Institute of Aeronautics and Astronautics

Following the design of the SUMR-13i rotor, the design of the 13.2 MW rotor will be further refined to result in a 25% reduction in the levelized cost of energy (LCOE) when compared to the CONR. The resulting 13.2 MW rotor will be named as the SUMR-13 rotor. It is important to note that this paper will focus on the aerodynamic design of the SUMR-13i rotor only where the aim of the overall design is to achieve a 25% reduction in the rotor mass when compared to the CONR while satisfying all technical and regulatory specifications based on the IEC standards.

III.   Design Tools

The design of the rotor itself can be divided into the design of the blade geometry and its individual airfoil sections. The aerodynamic design for the SUMR-13i followed the inverse-design approach where the desired aerodynamic performance parameters were prescribed and the corresponding geometry was obtained. The inverse design approach has an advantage over the direct-design approach where the number of iterations taken to obtain an optimized design geometry is considerably less. The direct-design approach may sometimes need a large number of iterations and can result in sub-optimal designs due to designer fatigue. The two in-house developed inverse design tools used for blade and airfoil design were PROPID[10,11] and PROFOIL,[12,13] respectively.

PROPID is an inverse design tool used to design the wind turbine rotor geometry itself. In PROPID, the desired performance from the rotor is specified via prescription of the rated power, operating tip speed ratio, average and rated wind speeds, axial induction distribution along the blade length, and the C_L distribution along the blade length, usually corresponding to the highest L/D of each of the airfoil cross-sections. Based on the aforementioned design parameters, the corresponding geometry of the rotor is obtained with specifications for the rotor diameter, blade pitch, and blade chord and twist distributions.

PROFOIL, which is also an inverse-design tool, is used for airfoil design. Here, the desired performance is set by prescribing the appropriate velocity profiles over the airfoil and the corresponding airfoil geometry is obtained. The airfoil geometry is then analyzed in XFOIL[14,15] and based on the performance of the designed airfoil the prescribed velocity profiles are adjusted again. The process is iterated to finally converge to an optimum airfoil design. Figure 2 illustrates the inverse-design methodology of PROFOIL and PROPID in a graphical manner.
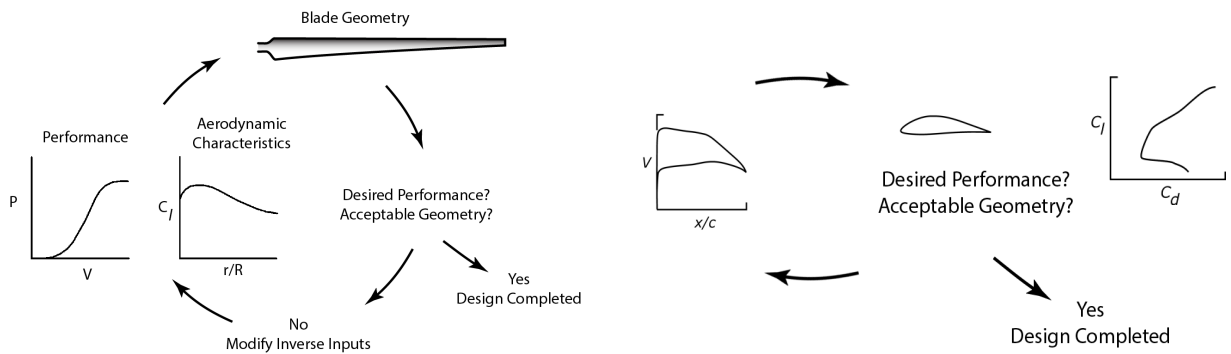

Figure 2. Inverse design tools methodology description: (a) PROFOIL for airfoil design and (b) PROPID for rotor design.

IV.   Design Process

The overall design process for the SUMR-13i rotor is outlined in the flowchart shown in Fig. 3. Once the system level requirements were identified, the necessary design specifications were set to meet those requirements. Some of the important considerations that underwent while deciding the required design specifications included a) the number of blades, b) upwind or downwind configuration, and c) specification of the variation of rotor coning angle with wind speed (henceforth referred to as coning angle schedule or morphing schedule).

American Institute of Aeronautics and Astronautics
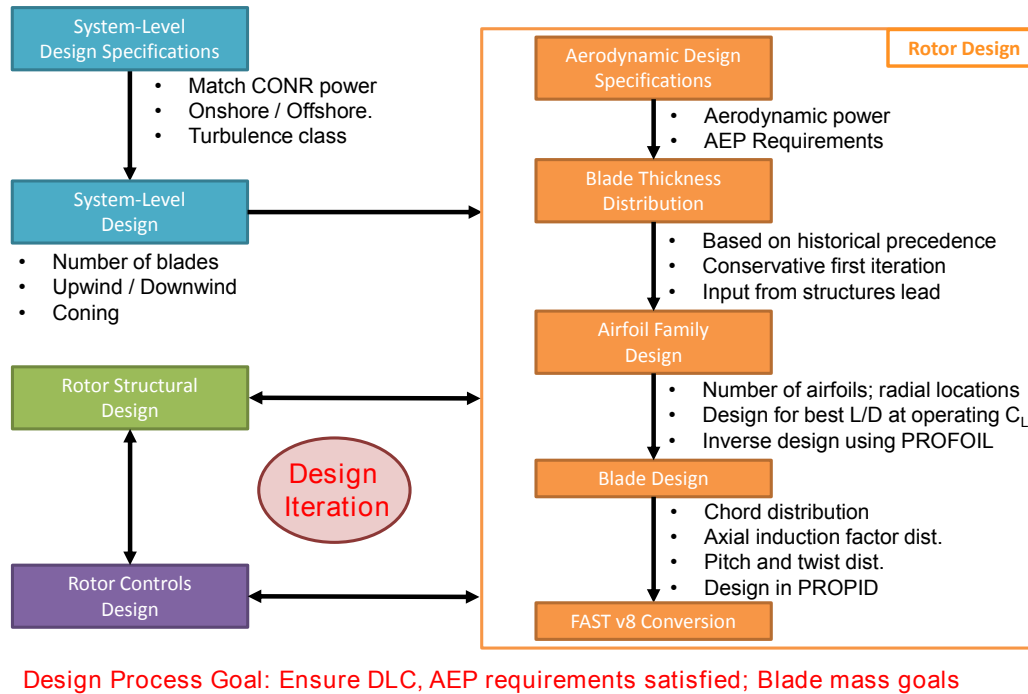
Figure 3. SUMR-13i rotor design process.

The actual rotor design process involved initially setting a blade thickness distribution based on historical precedence and input from the structures team. The thickness distribution set therefore provided input into the airfoils designed for the wind turbine blades. As previously discussed, airfoils were designed using PROFOIL with the goal of maximizing L/D at specific operating design lift coefficients. Once a set of airfoils were designed, the blade was designed using PROPID based on the design requirements set in Section II. The output from PROPID was a blade with a specific pitch, radius, and chord and twist distribution. The blade design and airfoil performance data was then converted to a format to be used in the FAST wind turbine blade dynamics code. In its current iteration, FAST v8, the FAST (Fatigue, Aerodynamics, Structures, and Turbulence) Code is a comprehensive aeroelastic wind turbine rotor simulator that has the ability of predicting the loads (extreme and fatigue) on horizontal-axis wind turbines (HAWTs).[16,17] With the aerodynamic design files as the inputs for FAST, the controls group implements various controllers in a bid to maximize power output at the average and rated speeds specified.[18,19] Together with the structures group, the goal of the controls group is to ensure that the designed rotor maintains safe load limits according to the IEC standards (International Electrotechnical Commision).[20] Therefore the goal of minimizing rotor mass is finally an iterative process between the aerodynamics, controls, and structures groups within the SUMR team.

V. Design Iterations

A.   Initial Blade Design Considerations

1. Tip Speed Ratio

While designing the wind turbines to operate at a higher tip speed ratio is desirable, higher tip speed ratios result in excess noise due to high tip velocities. Based on experience and historical precedence of operating wind turbines at offshore locations, the design tip speed ratio for the SUMR-13i rotor was selected to be 9.5.

American Institute of Aeronautics and Astronautics

2. Number of Blades

While most existing wind turbines are of a 3-bladed rotor configuration, the SUMR-13i was set to have a two-bladed rotor. The power output of a rotor is minimally dependent on the number of blades and is mainly dependent on the radius of the rotor. The difference in rotor C_P is also within 5% between a 2-bladed and 3-bladed rotor. As a result, the number of blades on the rotor does not have a major influence on the aerodynamic performance of the wind turbine. Hence, the decision to have two or three blades on the rotor was influenced by other factors such as controller considerations and the rotor weight. For instance, it is well-known that two-bladed wind turbine rotors experience fluctuating dynamic loading especially when yawing, and these cyclic loads impose significant stresses on various components of the wind turbines. However, having a two-bladed rotor instead of three typically results in a lighter rotor. With the staggering advances in controller design capabilities in recent times, it was decided to use a 2-bladed rotor along with a newly designed advanced controller to counteract the effects of the cyclic loads on the SUMR-13i rotor at these extreme-scales to reduce the overall mass of the rotor.

3. Rotor Orientation

The SUMR-13i rotor was selected to be of downwind configuration instead of upwind in order to avoid possible tower strikes and to allow for load alignment (as dicussed in Section I). The possibility of tower strikes in the upwind configuration will be greater for the SUMR-13i rotor because the blades are being designed to be thin and light which will result in greater blade flexibility and hence higher tip deflections. Having the rotor in the downwind configuration will help avoid the possibility of tower strikes, especially in case of sharp-gusts which are frequently encountered in the offshore locations.

4. Coning Angle

Finally, the manner in which the rotor coning angle will vary with wind speed (morphing schedule) will in turn determine the conditions at which the wind turbine aerodynamic design must be optimized. As mentioned earlier, the SUMR concept involves morphing a downwind rotor such that the combination of the centrifugal, gravitational, and aerodynamic loads are aligned with the blade axis in order to reduce the mean root bending moment. The morphing schedule is provided by the morphing team on the SUMR project using which the rotor coning angle at the rated speed is determined.[21] Once the coning angle at the rated speed is known, the SUMR-13i rotor was designed to operate in that morphing configuration optimally. The initial morphing schedule provided by the morphing team on the SUMR project is shown in Fig. 4. The coning schedule shows that from the cut-in wind speed, the SUMR-13i rotor will vary its cone angle until the average wind speed of 8.5 m/s is reached. From V_{avg} onward, the coning angle is maintained at 12.5 deg. It is important to note that the simplified morphing schedule shown in Fig. 4 is not complete and does not account for morphing at wind speeds much higher than the rated speed.
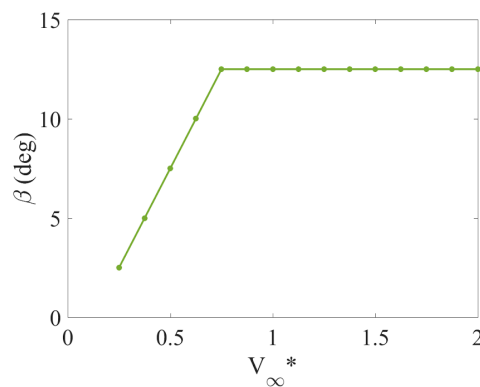

Figure 4. SUMR-13i coning schedule where $V_\infty*$ is V/V_{rated}.[21]

American Institute of Aeronautics and Astronautics

B. Airfoil Design

Once the aerodynamic parameters from the system level requirements were determined, the rotor aerodynamic design process started by designing the airfoils to be used at the various wind turbine blade cross-sections. The airfoils were designed to achieve the desired blade thicknesses at the corresponding radial blade locations. The blade thickness at a given radial blade location was set based on historical precedence [CONR wind turbine (SNL 100-03 blades) and 50 m blades with flatback airfoils]. The thickness distribution analysis comparisons with the other blades is shown in Fig. 5.

Based on the expected size of the rotor to produce 13.2 MW rotor ($R = 100$ m), the operating tip speed ratio (TSR = 9.5), and the average and rate speeds ($V_{avg} = 8.5$ m/s, $V_{rated} = 11.3$ m/s), a range of Reynolds number was estimated. The SUMR-13i wind turbine rotor blades were expected to operate within a range of Reynolds number varying from 4,000,000 toward the hub to as high as 15,000,000 near the tip. Therefore, to leverage the best aerodynamic performance from the airfoils at such high Reynolds numbers combined with various structural requirements, a series of flatback airfoils were designed in PROFOIL.

The preference of choosing flatback airfoils over conventional airfoils resulted from high blade-thickness requirements. Conventional airfoils with sharp trailing edges when designed for high thickness can result in separated flow and hence sub-optimal aerodynamic performance. The flow separation for sharp-trailing edge airfoils with high thickness occurs as a result of higher suction peak on the airfoil due to higher airfoil thickness which results in a higher adverse pressure gradient. Flatback airfoils allow generation of high suction peaks while reducing the adverse pressure gradients by having blunt trailing edges to reduce the pressure recovery requirements, thus allowing the airfoil to be thick and perform well at the same time. When operating at high Reynolds number range of 4,000,000–15,000,000, well-designed flatback airfoils can produce a $C_{l_{max}}$ greater than 2.0 depending on the thickness of the airfoil and a maximum C_l/C_d of nearly 200. Having high C_l/C_d at high values of C_l results a smaller rotor radius thus resulting in
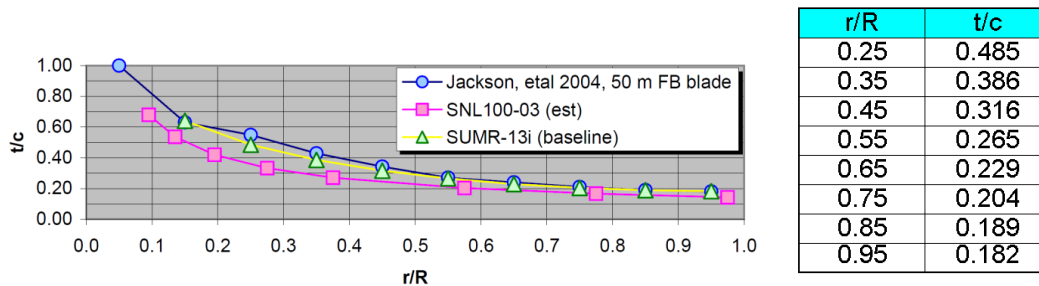

r/R	t/c
0.25	0.485
0.35	0.386
0.45	0.316
0.55	0.265
0.65	0.229
0.75	0.204
0.85	0.189
0.95	0.182

Figure 5. SUMR-13i blade thickness distribution.

r/R	t/c
0.25	0.485
0.35	0.386
0.55	0.265
0.75	0.204
0.95	0.182

F1-4846-1226

F1-3856-0738

F1-2655-0262

F1-2040-0087

F1-1822-0041

Figure 6. SUMR-13i F1 airfoil family.

American Institute of Aeronautics and Astronautics
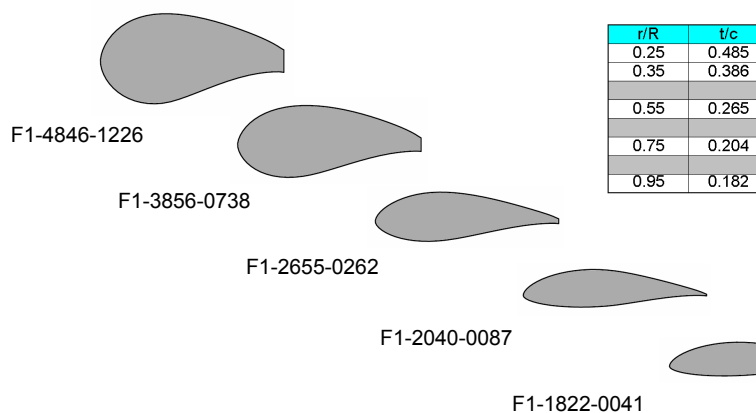
lower rotor mass and higher rotor aerodynamic efficiency.

In PROFOIL, the desired velocity distribution, thickness, and moment requirements were set a-priori. The F1 family of airfoils were then designed as shown in Fig. 6 to be used on the 13.2 MW SUMR rotor blades. The airfoils have a maximum thickness varying from 18 percent toward the tip to as high as 48 percent near the hub. Similarly, the trailing edge thickness on the F1 series airfoils will vary from 0.4 percent toward the tip to as high as 12.26 percent near the hub. The naming convention for the F1 family of airfoils is given by F1-AAAA-BBBB, where 'AAAA' derives from the maximum thickness of the airfoil ($t/c_{max} \times 10,000$) and 'BBBB' derives from the trailing edge thickness of the airfoil ($t/c_{TE} \times 10,000$).

Given that the F1 series airfoils will operate in a high Reynolds number regime with the Reynolds number at the tip approaching a value of 15,000,000, the accuracy of the tools being used to obtain airfoil data needs to be inspected. It is well known already that having accurate airfoil data has a significant impact on the accuracy of results obtained from any kind of tool that use the Blade Element Momentum (BEM) method. Since PROPID is a BEM-based inverse design tool, it becomes important to analyze various commonly used methods and tools to obtain airfoil data. Such an investigation into the accuracy of commonly used airfoil analysis tools is especially important for the F1 series airfoils because of their high thicknesses and large blunt trailing edges and due to the fact that they are being designed to operate in a high Reynolds number regime.

Wind tunnels capable of achieving a Reynolds number as high as 15,000,000 are not commonly available and hence obtaining high quality airfoil data from wind tunnel tests for the F1 series airfoils was not possible. Instead, commonly available computational tools with varying degree of fidelity ranging from a lower-order tool such as XFOIL to a higher-fidelity method such as CFD with RANS-based laminar-to-turbulent transition simulation capability were used to obtain the airfoil data. In order to determine which tool is more accurate in comparison with the other, XFOIL and ANSYS Fluent were compared with the wind tunnel test data[22] at a Reynolds number of 15,000,000 obtained for an extreme-scale 10 MW wind turbine airfoil, DU00-W-212[22] with 21 percent thickness. The wind tunnel tests were performed in the DNW-HDG pressurized wind tunnel as a part of the AVATAR project[23] with an aim to validate aerodynamic analysis tools for extreme-scale wind turbines.

ANSYS Fluent is a finite-volume based commercial Reynolds-Averaged Navier-Stokes (RANS) equations solver. The simulation of laminar-to-turbulent boundary layer transition is critical for obtaining better aerodynamic performance of an airfoil. Hence, the Transition SST turbulence model[24] was used for computations in ANSYS Fluent. The Transition SST model is a two equation shear-stress transport (SST) k-ω model coupled with two additional transport equations for intermittency γ and transition momentum thickness Reynolds number Re_{θ_t} for prediction of boundary layer transition based on empirical correlations. The model calculates the transition onset Reynolds number Re_{θ_t} in the freestream using empirical correlations which is then diffused into the boundary layer. The transition onset Reynolds number in the boundary layer is subsequently used by the transition onset criteria in the intermittency transport equation, where intermittency is used to trigger transition by allowing production of turbulent kinetic energy downstream of the transition onset location. The Transition SST method does not model the actual physics of the transition. The
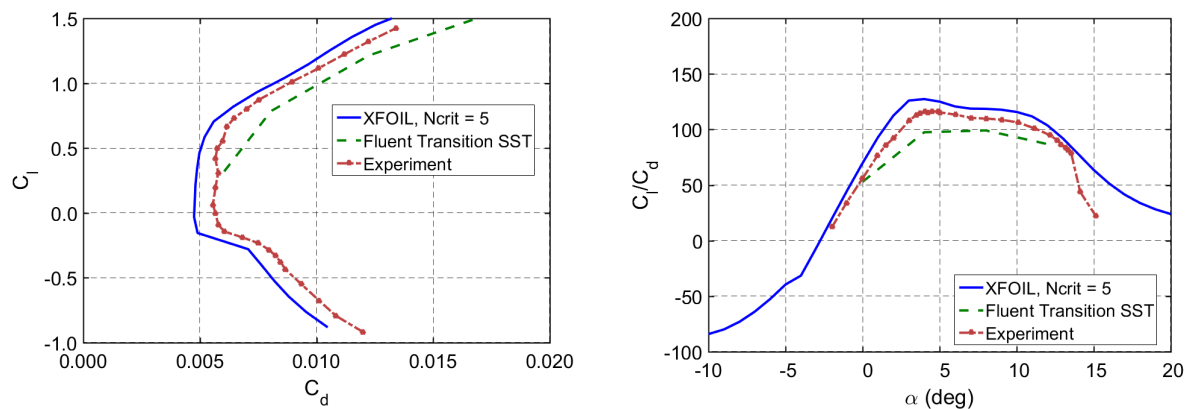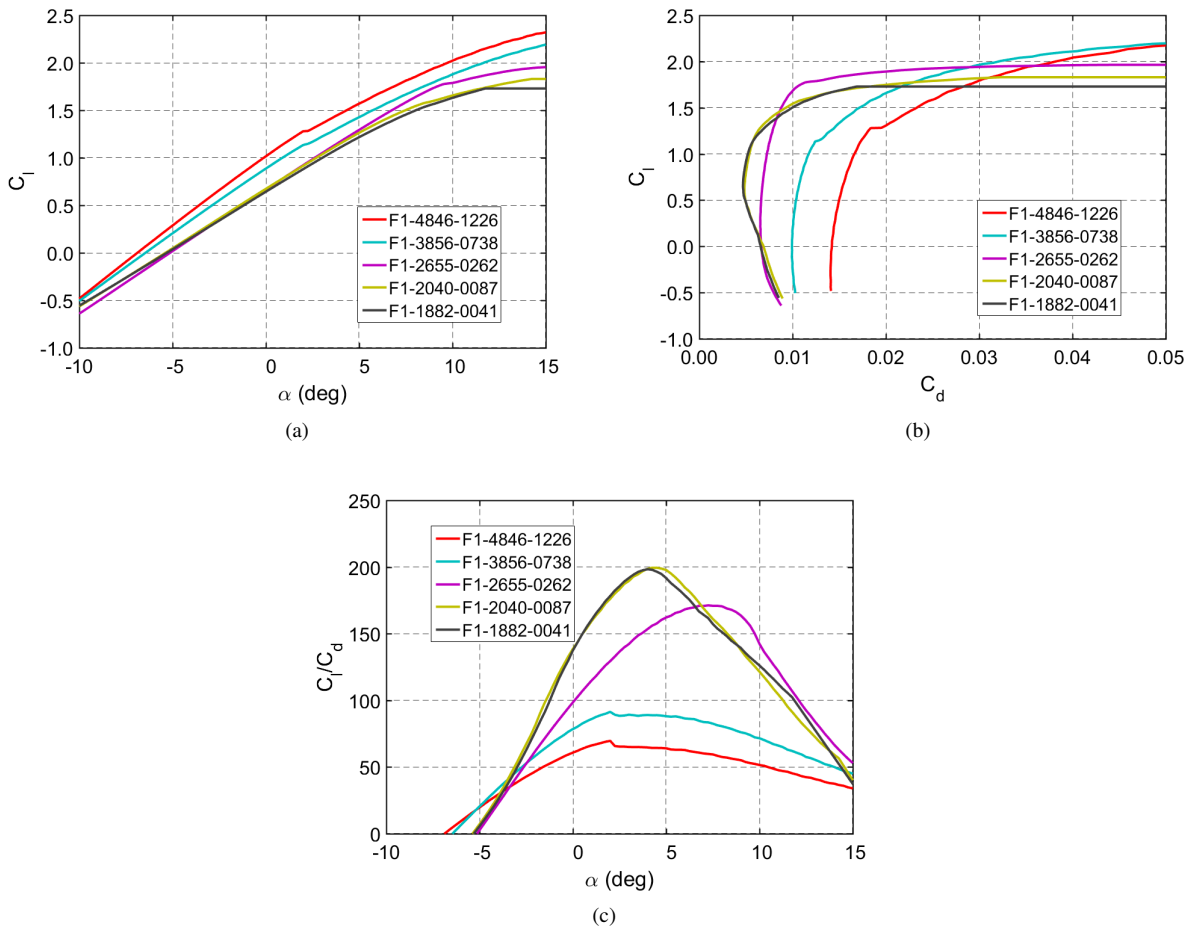

Figure 7. Comparison of airfoil data predictions for the DU00-W-212 airfoil at $Re = 15,000,000$ **from ANSYS Fluent Transition SST model and XFOIL with experimental results[22]: (a)** C_l **vs** C_d **and (b)** C_l/C_d **vs** α.

American Institute of Aeronautics and Astronautics

Figure 8. Airfoil data from XFOIL for the F1 series flatback airfoils showing: (a) C_l **vs** α**, (b)** C_l **vs** C_d**, and (c)** C_l/C_d **vs** α**.**

physics of the transition process is contained within the empirical correlations that the model uses.

The comparison of results from ANSYS Fluent and XFOIL have been performed with the experimental data at a Reynolds number of 15,000,000 and a turbulent intensity of 0.33 percent[22] and is shown in Fig. 7. The N_{crit} value corresponding to a turbulent intensity of 0.33 percent used in XFOIL was 5.28 and was determined using the Mack's empirical relation as shown.

$$N_{\text{crit}} = -8.43 - 2.4\ln(Ti) \tag{1}$$

Figure 7 shows that the e^N transition method with an N_{crit} value of 5 in XFOIL performed better than ANSYS Fluent with Transition SST model when compared with the experimental results. Running XFOIL at a lower N_{crit} causes early flow transition on the airfoil and hence results in a higher drag and lower C_l/C_d. Despite running XFOIL at an N_{crit} value of 5 corresponding to the turbulence intensity of 0.33 percent in the wind tunnel test section, it underpredicted C_d and overpredicted C_l/C_d when compared to the experimental data.

Based on the above analysis, XFOIL was selected as the airfoil analysis tool for the SUMR-13i design. The aim of using XFOIL was to obtain accurate F1 series airfoil data for a Reynolds number range of 4,000,000 – 15,000,000 and freestream turbulence of 0.07 percent in a good wind tunnel (which corresponds to $N_{\text{crit}} = 9$ in XFOIL). However as seen earlier, XFOIL had a tendency to overpredict C_l/C_d and underpredict C_d which may have a significant impact on the rotor design. Hence, it was decided to obtain data for the F1 series airfoils using XFOIL with an N_{crit} value of 6 (less than 9) to promote transition early on the airfoil, thus predicting higher C_d and lower C_l/C_d. Hence, running XFOIL at a lower N_{crit} value should compensate for its tendency to overpredict C_l/C_d and hence lead to more accuracy. The airfoil data used in the design of the 13.2 MW SUMR rotor is shown in Fig. 8.

C. Initial Blade Design

1. Baseline

Based on the requirements set for the SUMR-13i in Section II, the initial blades were designed to a rated aerodynamic power of 13.9 MW (assuming 95% generator efficiency) at a rated wind speed of 11.3 m/s. Additional inputs into PROPID include setting the axial induction factor distribution to the Betz limit of 1/3 along the entire blade when operating at a tip speed ratio of 9.5 as shown in Fig. 9(a). Finally, the initial lift coefficient distribution was set to a C_L range that started at 1.25 at r/R of 0.25 and linearly decreased to a C_L of 0.9 at r/R of 0.95. The lift distribution set for the blade is shown in Fig. 9(b).

The designed SUMR-13i_v1 (baseline) blade was with a rotor radius of 99.96 m and had a C_P of 0.4998 at V_{avg} = 8.5 m/s and tip speed ratio of 9.5. The optimal pitch of the blade was set to 2.62 deg, and the rotor operated at 7.74 and 10.29 RPM at average and rated speeds respectively. The chord ratio, twist, lift-to-drag ratio, and operating Reynolds number of the SUMR-13i_v1 blade at V_{avg} is shown in Fig. 10. At steady state conditions, based on a Weibull wind speed distribution of k = 2 and γ = 0.8862, the AEP calculated was 53,674 MWh/yr/turbine.

2. Trade Study: 2 vs 3 blades

To verify the choice of a two-bladed wind turbine rotor, a trade study was performed on the SUMR-13i_v1 baseline design. The trade study involved designing the rotor under the same conditions and for same design parameters using two and three blades and comparing their design specifications and performance. The resultant blade properties comparison is shown in Fig. 11 where the white line refers to the SUMR-13i_v1 two-bladed configuration and the green line refer to the three-bladed configuration. The resultant three-bladed design shows a reduction of 1.6% in
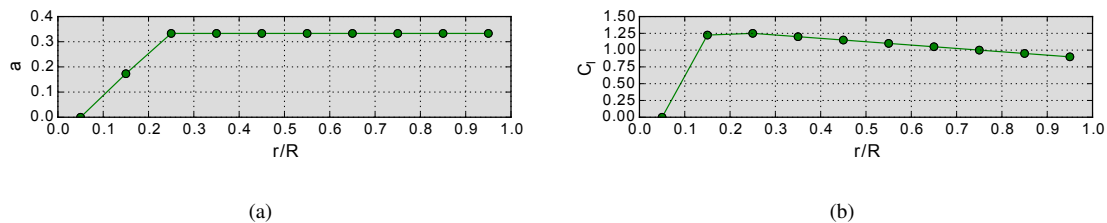
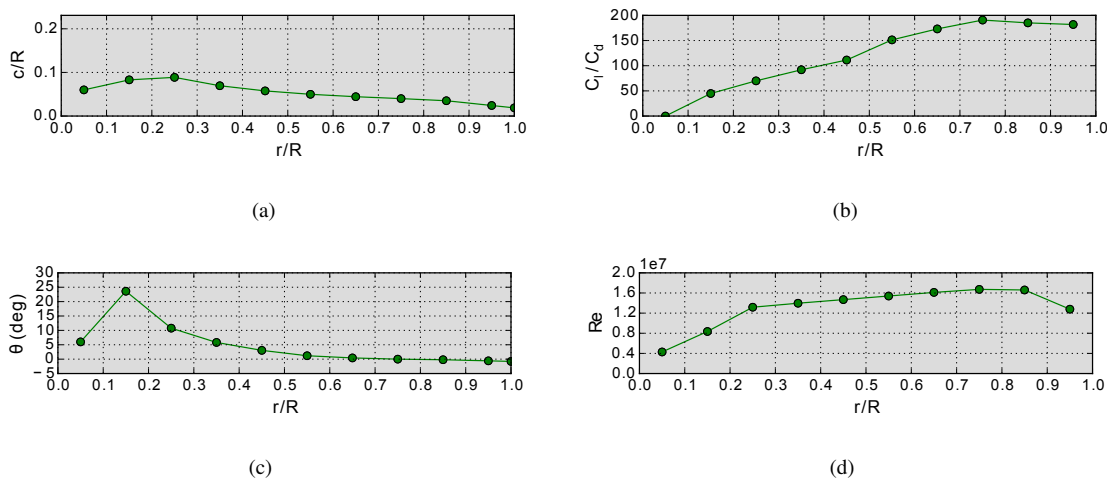**Figure 9. SUMR-13i_v1 baseline blade parameters (a) axial induction and (b) Cl distribution.**

Figure 10. SUMR-13i_v1 baseline blade design details (a) chord distribution, (b) lift-to-drag ratio distribution, (c) twist distribution, and (d) Reynolds number distribution.
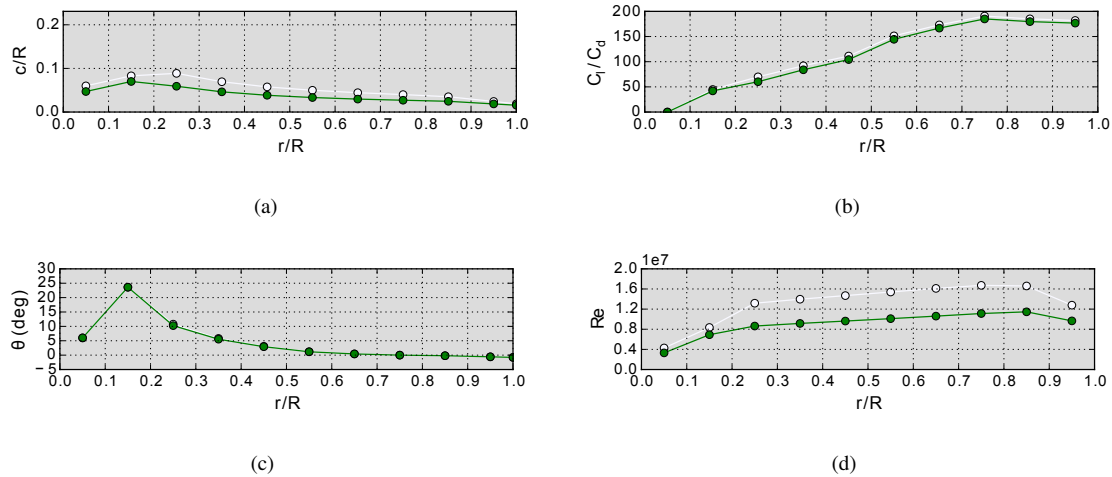
American Institute of Aeronautics and Astronautics

(a)

(b)

(c)

(d)

Figure 11. SUMR-13i_v1 baseline blade number trade study (2-bladed – white, 3-bladed – green) (a) chord distribution, (b) lift-to-drag ratio distribution, (c) twist distribution, and (d) Reynolds number distribution.

radius to 98.3 m. From Fig. 11(a), it is evident that the chord distribution on the blades of the 3-bladed rotor is less than the two-bladed rotor. In addition, as discussed earlier, a 3.3% increase in C_P is observed. However, a comparison of AEP between the two designs shows a negligible difference. With no effect on the AEP and minimal difference between the maximum C_P values between the two and three-bladed rotor, it can be safely concluded that the choice of a two or three bladed rotor for the SUMR-13i is not strongly influenced by aerodynamic considerations. Therefore, with the rotor mass and LCOE as the driving objectives, it was decided to have two blades on the SUMR-13i rotor.

3. *Trade Study:* TSR *of 9.5 vs 8.5*

Selection of the optimum operating tip speed ratio for a variable speed turbine is important. Hence, an additional trade study for selection of the optimal tip speed ratio was conducted. Figures 12(a–d) show the blade design comparisons for the rotor with a TSR of 9.5 (white) and 8.5 (green). From these plots it can be observed that the blade corresponding to a lower tip speed ratio has a larger chord. A decrease in tip speed ratio from 9.5 to 8.5 results in an increase of C_P
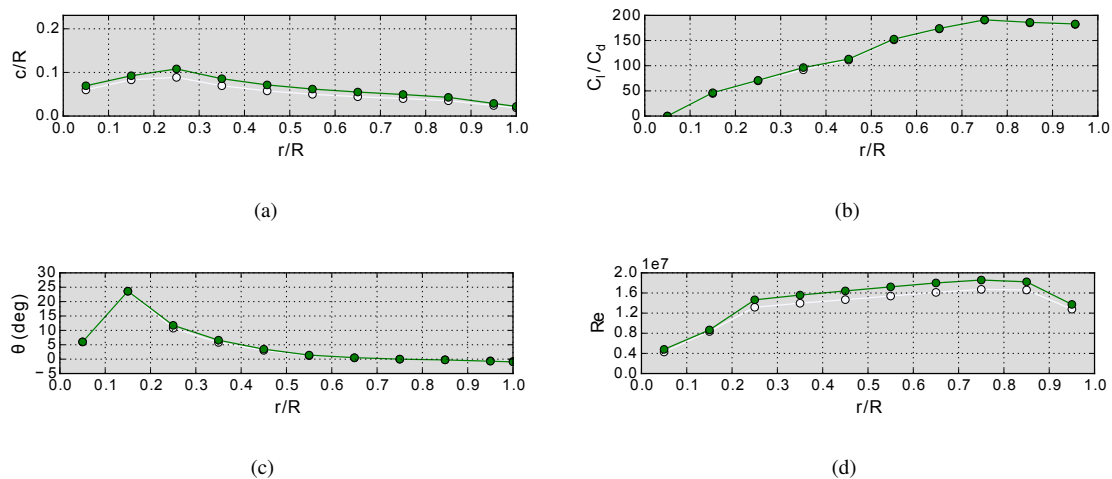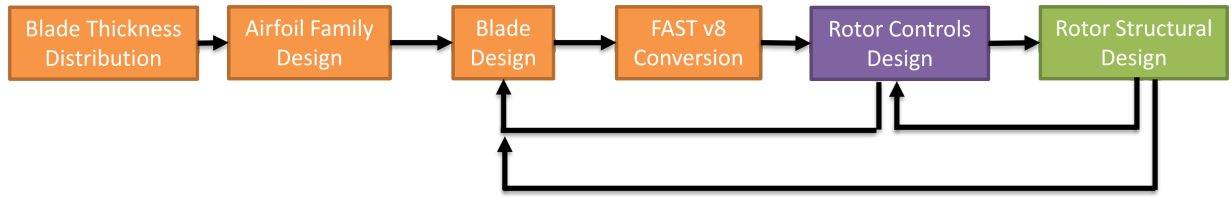

(a)

(b)

(c)

(d)

Figure 12. SUMR-13i_v1 baseline blade design details (a) chord distribution, (b) lift-to-drag ratio distribution, (c) twist distribution, and (d) Reynolds number distribution.

American Institute of Aeronautics and Astronautics

Figure 13. SUMR-13i blade design process iterations.

of 0.5%, increase of radius of 0.3%, and an increase in the chord distribution. It can be concluded from these results that to reduce the mass of the rotor a higher tip speed ratio should be selected. Although operation at a higher TSR is desirable, the operating TSR was limited to 9.5 to prevent excessive noise due to higher tip speeds.
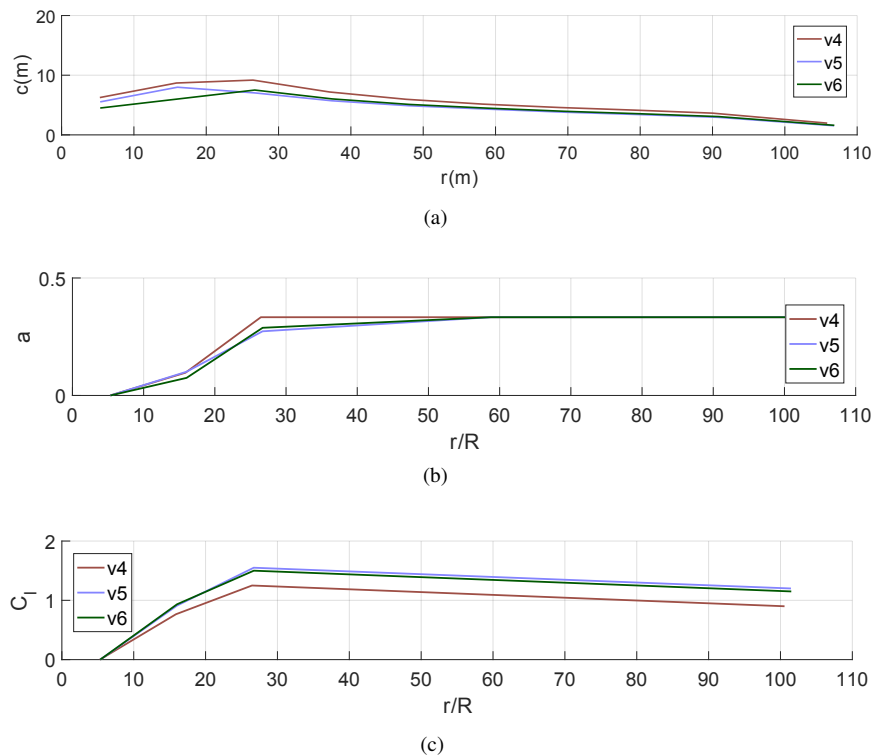
D. Blade Design Iterations

Once the initial aerodynamic design was performed, the design was delivered to the structures and the controls teams. Based on the simulation results from the structures and controls teams, relevant recommendations were made to modify the aerodynamic design, thus forming an iterative loop. During each iteration step, feedback was taken from both controls and structural design groups to ensure that the DLC and AEP requirements were met within the FAST v8 framework as shown in Fig. 13.

Table 2 lists all the critical blade details of the CONR and the v4, v5, and v6 iterations of the SUMR-13i blade. Although there were 6 iterations of the SUMR-13i design, only the last three versions are discussed in this Section. Iterations v2 and v3 for the SUMR-13i were done to ensure that the design process with both controls and structures were performed smoothly. As shown in Table 2, the final blade length for the SUMR-13i was 106.85 m with a rated rotation speed of 9.55 RPM.

The SUMR-13i_v4 design was designed based on a design C_l of 1.0 at the 75% blade span location. As shown in

Table 2. CONR and SUMR-13i Blade Design Details

Metric	CONR	SUMR-13i_v4	SUMR-13i_v5	SUMR-13i_v6
Geometry				
Rotor Radius (m)	102.5	105.86	106.80	106.85
Direction	Upwind	Downwind	Downwind	Downwind
Number of Blades	3	2	2	2
Coning Angle (deg)	2.5	12.5	12.5	12.5
ω @ 8.5 m/s (RPM)	7.46	7.46	7.19	7.18
ω @ 11.3 m/s (RPM)	9.77	9.92	9.55	9.55
Pitch Angle (deg)	0	2.50	0	0.48

American Institute of Aeronautics and Astronautics

Figure 14. SUMR-13i design iteration blade (a) chord, (b) axial induction, and (c) Cl distribution.

Fig. 14(c), the desired C_l for the blade was linearly increased towards the blade hub and decreased towards the blade tip. The linear tapering of the C_l distribution on the blade was done such that C_l at each airfoil section corresponded to a high C_l/C_d value. In addition, a desired axial induction of 0.333 was enforced from the 25% blade span to the tip as shown in Fig. 14(b). A blade with a 105.86 m radius resulted to acheive a 13.89 MW rotor power at the rated wind speed of 11.3 m/s.

Based on feedback from structures team, it was realized that the designed blade could not achieve the specified blade mass goals. As a result, a trade study was performed looking at the variation of design C_l and axial induction in a bid to reduce blade mass. The result of the trade study is the SUMR-13i_v5 blade. This blade is designed based on a design C_l of 1.3 at the 75% blade span location as shown in Fig. 14(c). The slope of the linear variation of C_l along the blade was maintained to be similar to the SUMR-13i_v4. In addition, the 0.333 axial induction factor enforcement close to blade hub was relaxed as shown in Fig. 14(b) allowing for a reduction in chord close to the blade hub. The axial induction factor was set to 0.25, 0.29, and 0.31 at the r/R locations of 0.25, 0.35, and 0.45 respectively. The result of these changes increased the blade length to 106.8 m but also reduced the blade chord distribution by an average of 20-25% from the v4 design.

The final change in the blade design in v6 was decreasing the blade design C_l at the 75% blade span location to 1.25 based on feedback from the structures team to increase the overall chord slightly [see Fig. 14(c) and 14(a)]. In addition, the maximum chord location was shifted to the 25% blade span location and the hub diameter was fixed at 4.5 m. These changes further decreased the overall blade mass and achieved the required 25% blade mass goal compared with the CONR rotor design configuration. The final blade radius for the SUMR-13i was 106.85 m and had a pitch of 0.48 deg.

A comparison of C_P as a function of TSR for the CONR and SUMR-13i blade designs is shown in Fig. 15. The plot shows that the SUMR blade designs maintain C_{Pmax} at the tip speed ratio of 9.5 and these are comparable to the CONR rotor C_{Pmax}. The final SUMR-13i (SUMR-13i_v6) design specifications are shown in Table 3.
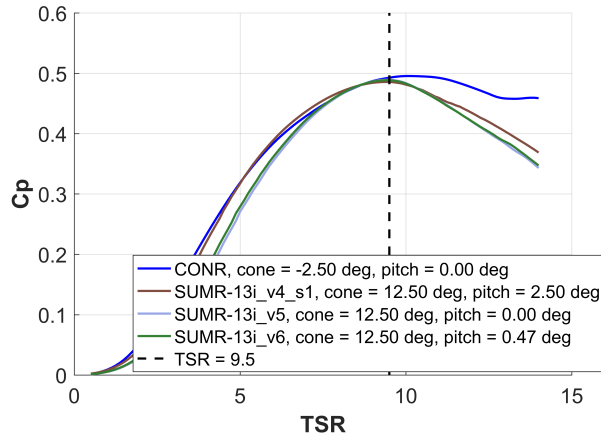
American Institute of Aeronautics and Astronautics

Figure 15. CONR and SUMR-13i C_P vs TSR curves.

VI. Blade Loading in Operation

With the final SUMR-13i_v6 design complete, it was necessary to understand the loading of the blades in operation based on the various cone angle settings. When the rotor is morphed to cone at a certain angle, the forces contributing to the net force perpendicular to the blade axis are the 1) aerodynamic thrust loads, 2) centrifugal loads, and 3) gravitational loads. The manner in which forces act to cause a resultant root bending moment is depicted in Fig. 16.

Figures 17–18 depict the loads on the blades for coning angles ranging from 0 to 30 deg at the rated wind speed of 11.3 m/s and the design tip speed ratio of 9.5. The aerodynamic loads were obtained using BladeMorph, [25,26] a BEM-based computational tool developed for analysis of SUMR wind turbine rotors. Figure 17 illustrates the contribution of each blade element toward the total blade loading and the resulting root bending moment.

From Fig. 17(a) it can be observed that with higher coning the component of gravitational load acting normal to the blade increases, especially near the root where the blade is the heaviest. The component of the centrifugal force normal to the blade also increases significantly with higher coning, as shown in Fig. 17(b). The blade elements at the center of the blades contribute the highest portion of the centrifugal loads in the blade-normal direction. The center blade elements contribute the highest because even though the radius at the tip is larger than the center of the blade, the mass at the tip is lesser than that at the center which results in lower contribution of centrifugal loads from the tip region elements. While the gravitational and centrifugal components of the net load in the blade-normal direction became larger at higher coning angles, the aerodynamic thrust loads decreased as the cone angle was increased, as

Table 3. SUMR-13i Final Design

Metric	CONR	SUMR-13i
Rated Power (P_{rated})	13.2 MW	13.2 MW
Avg. Wind Speed (V_{avg})	8.5 m/s	8.5 m/s
Rated Wind Speed (V_{rated})	11.3 m/s	11.3 m/s
Cut-out Wind Speed ($V_{cut-out}$)	25 m/s	25 m/s
Rotor Radius (R)	102.5 m	106.85 m
Rated Rotor Speed (Ω)	7.44 RPM	9.54 RPM
Tip-Speed Ratio (TSR)	9.66	9.5
Rotor Orientation	Upwind	Downwind
Number of Blades (B)	3	2
Cone Angle (β)	-2.5 deg	2.5 to 12.5 deg
Blade Mass (m_{blade})	49,519 kg	55,700 kg
Rotor Mass (m_{rotor})	148,500 kg	111,400 kg

shown in Fig. 17(c). On comparison of the three loads separately in Fig. 17, it can be observed that the aerodynamic thrust generated on the rotor was significantly higher than the gravitational and centrifugal loads. Hence, as the rotor
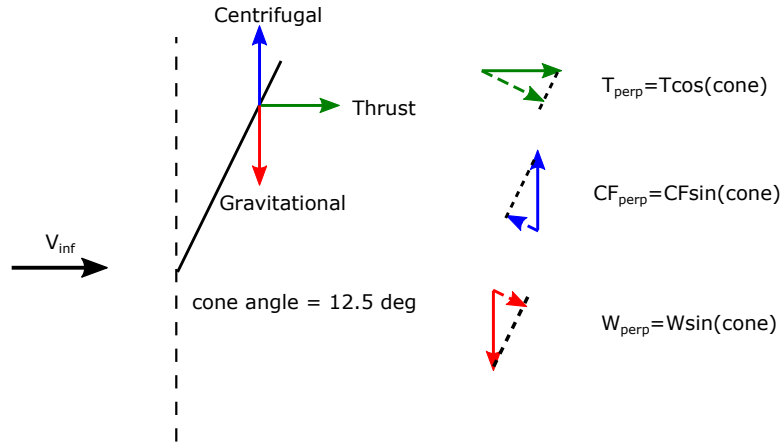

Figure 16. Free body diagram depicting forces contributing to the blade in the direction perpendicular to the blade when coned.
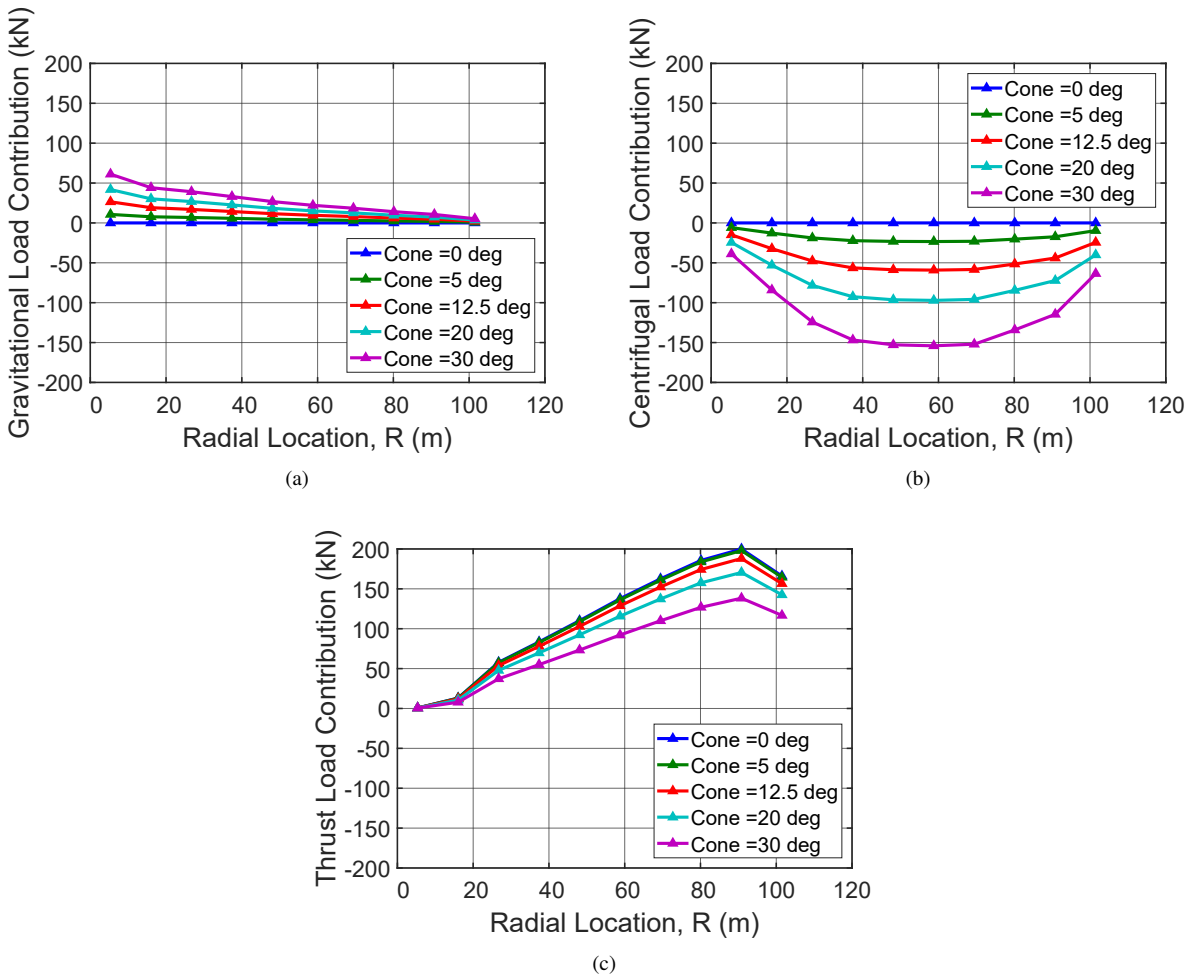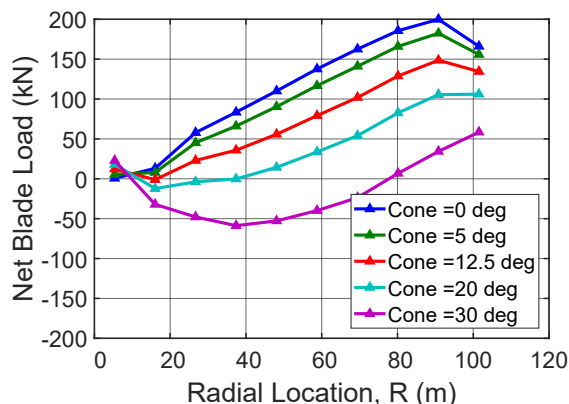

(a)

(b)

(c)

Figure 17. Axial blade loading at the rated conditions on the SUMR-13i rotor for coning angles ranging from 0 − 30 deg showing: (a) gravitational load component, (b) centrifugal load component, and (c) aerodynamic thrust load component.

American Institute of Aeronautics and Astronautics

Figure 18. Net force in the blade-normal direction from each blade element at the rated conditions on the SUMR-13i rotor for coning angles ranging from 0 – 30 deg.

is morphed to a higher angle, the overall effect is a reduction in the net load perpendicular to the blades with coning angle, which also causes the root bending moment to decrease, as shown in Fig. 18.

Although Fig. 18 shows that higher coning is better for reduced net blade-normal direction force (and correspondingly root flapwise bending moment), coning the rotor at a higher angle results in lower rotor swept area which leads to generation of lower aerodynamic power. To achieve the same aerodynamic power by coning the rotor to achieve lower root flapwise bending moment, the blades must be made longer which in turn increases their mass. Hence, there is a tradeoff in the coning angle chosen for reducing the blade root bending moment to generate the same aerodynamic power. The aforementioned analysis shows that perfect load alignment where the net forces are totally aligned with the blade axis may not result in a feasible rotor design. However, morphing the rotor at smaller coning angles results in a balance between the desired power generation and lower root flapwise bending moments, thereby resulting in a lower blade mass.

VII.   Conclusions

The ARPA-E funded SUMR program intends to address and overcome various technical and economical challenges associated with the design of extreme-scale offshore wind turbines (up to 50 MW) using the conventional method. In order to deal with the structural and weight constraints for the rotor blades at such extreme scales, the SUMR concept was proposed for load alignment to reduce blade mass for an ultralight blade design. In order to achieve this aim, an offshore, downwind, two-bladed, horizontal-axis, 13.2 MW wind turbine rotor was designed based on the SUMR concept.

The design study began by identifying the system-level requirements for the SUMR-13i wind turbine such as the ultimate aim of the design, rated capacity of the turbine, selection of offshore location where the turbine will be operated, number of blades, rotor configuration (upwind or downwind), and the operating tip speed ratio.

The initial design process of the SUMR-13i rotor started with the design of the airfoils for the rotor blades. A new set of flatback airfoils (F1-series) were designed with high thickness to satisfy the structural constraints. The flatback airfoils were designed to operate at high Reynolds number range of 4,000,000 – 15,000,000 with Cl_{max} greater than 2.0 and a maximum C_l/C_d of nearly 200, depending on the thickness of the flatback airfoil. In order to obtain high quality airfoil data for these thick flatback airfoils with large blunt trailing edges at a high Reynolds number range of 4,000,000 – 15,000,000, XFOIL and the Transition SST model in ANSYS Fluent were compared against experimental data for the DU00-W-212 airfoil at Reynolds number of 15,000,000. It was found that XFOIL overpredicted C_l/C_d and Transition SST model underpredicted the same when compared to the experimental results for the same turbulence intensity. XFOIL was selected as the airfoil analysis tool primarily due to its rapid analysis capability. To compensate for the tendency of XFOIL to overpredict C_l/C_d and underpredict C_d, it was decided to run XFOIL with a lower N_{crit} value than the default value of 9 to promote early transition on the airfoils.

Once the airfoils were designed an initial baseline SUMR-13i_v1 rotor was designed. Trade studies were performed

American Institute of Aeronautics and Astronautics

to inspect the influence of the number of blades and the tip speed ratio on the aerodynamic performance of the rotor. It was found that designing a rotor under same conditions and for same design parameters but with two or three blades did not have a major impact on the maximum C_P value or the annual energy production. Hence, two-bladed rotor configuration was selected for the SUMR-13i rotor in order to reduce rotor mass. It was also found that designing the rotor for a lower tip speed ratio of 8.5 when compared to a TSR of 9.5 did not have any major impact on the maximum C_P value or the annual energy production. However, the rotor design for the TSR of 8.5 resulted in larger radius and bigger chord distribution which would have led to an increase in the rotor mass. Hence, a higher TSR was selected and limited to 9.5 due to noise constraints.

Based on the system-level requirements, trade-study results, and the provided morphing schedule, the aerodynamic design of the rotor was performed to optimize its performance at the rated speed of 11.3 m/s to produce a rated power of 13.2 MW at a coning angle of 12.5 degrees. The aerodynamic design was subsequently passed on to the structures and controls group in the SUMR team to analyze the performance of the rotor design from structural and controller perspective. Based on their results, recommendations were made based on which the aerodynamic design was further modified to meet the structural and controller requirements, thus forming a design loop. The final design occurred at the sixth design iteration and resulted in a rotor radius of 106.85 m and a pitch of 0.48 deg.

Finally, it was found that coning the rotor to completely align the blade loads with the blade axis to reduce blade flapwise bending moments may not result in a feasible design. Complete alignment of blade loads with the blade axis resulted in designing the rotor to operate at a higher cone angle. Operation at a higher coning angles result in a requirement for a larger blade which in turn adds mass to the rotor. Hence, there exists a tradeoff where the morphing schedule was selected such that the blade loads were partially aligned with the blade axis which resulted in lower root flapwise bending moments while at the same time maximizing the power produced by the rotor.

VIII.   Acknowledgment

References

[1]U.S. Department of Energy, "Wind Vision: A New Era of Wind Power in the United States," http://energy.gov/eere/wind/wind-vision, 2017–.

[2]Advanced Research Projects Agency-Energy (ARPA-E), "50 MW Segmented Ultralight Morphing Rotors for Wind Energy," https://arpa-e.energy.gov/?q=slick-sheet-project/ultra-large-wind-turbine, 2015–.

[3]Sandia National Laboratories, "Enormous blades could lead to more offshore energy in U.S," https://share.sandia.gov/news/resources/news_releases/big_blades/#.WBc2qugrJaS, 2016–.

[4]Steele, A., Ichter, B., Qin, C., Loth, E., Selig, M. S., and Moriarity, P. J., "Aerodynamics of an Ultralight Load-Aligned Rotor for Extreme-Scale Wind Turbines," AIAA Paper 2013-0914, Grapevine, Texas, 2013.

[5]Loth, E., Ichter, B., Selig, M. S., and Moriarty, P. J., "Downwind Pre-Aligned Rotor for a 13.2 MW Wind Turbine," AIAA Paper 2015-1661, 33rd Wind Energy Symposium, AIAA Scitech, Kissimmee, Florida, January 2015.

[6]Ichter, B., Steele, A., Loth, E., and Moriarty, P. J., "Structural Design and Analysis of a Segmented Ultralight Morphing Rotor (SUMR) for Extreme-Scale Wind Turbines," AIAA Paper 2012-3270, 42nd AIAA Fluid Dynamics Conference and Exhibit, New Orleans, Louisiana, June 2012.

[7]Loth, E., Steele, A., Qin, C., Ichter, B., Selig, M. S., and Moriarty, P., "Downwind pre-aligned rotors for extreme-scale wind turbines," *Wind Energy*, Vol. 20, No. 7, July 2017, pp. 1241–1259.

[8]Griffith, D. T. and Ashwill, T. D., "The Sandia 100-meter All-Glass Baseline Wind Turbine Blade: SNL100-00," Tech. Rep. SAND2011-3779, Sandia National Laboatories Technical Report, June 2011.

[9]Griffith, D. T. and Richards, P. W., "The SNL100-03 Blade: Design Studies with Flatback Airfoils for the Sandia 100-meter Blade," Tech. Rep. SAND2014-18129, Sandia National Laboatories Technical Report, September 2014.

[10]Selig, M. S. and Tangler, J. L., "Development and Application of a Multipoint Inverse Design Method for Horizontal Axis Wind Turbines," *Wind Engineering*, Vol. 19, No. 5, 1995, pp. 91–105.

[11]Selig, M. S., "PROPID – Software for Horizontal-Axis Wind Turbine Design and Analysis," http://www.ae.illinois.edu/m-selig/propid.html, 1995–.

[12]Selig, M. S. and Maughmer, M. D., "Generalized Multipoint Inverse Airfoil Design," *AIAA Journal*, Vol. 30, No. 11, 1992, pp. 2618–2625.

[13]Selig, M. S., *Multi-Point Inverse Design of Isolated Airfoils and Airfoils in Cascade in Incompressible Flow*, PhD dissertation, Dept. of Aerospace Engineering, Pennsylvania State Univ., University Park, PA, May 1992.

[14]Drela, M., "Viscous-Inviscid Analysis of Transonic and Low Reynolds Number Airfoils," *AIAA Journal*, Vol. 25, No. 10, 1987, pp. 1347–1355.

[15]Drela, M., "XFOIL: An Analysis and Design System for Low Reynolds Number Airfoils," *Low Reynolds Number Aerodynamics*, edited by T. J. Mueller, Vol. 54 of *Lecture Notes in Engineering*, Springer-Verlag, New York, June 1988, pp. 1–12.

[16]Jonkman, J. M. and Buhl Jr., M., "FAST User's Guide," Tech. Rep. NREL/EL-500-38230, National Renewable Energy Laboratory, 1617 Cole Boulevard, Golden, Colorado, Aug 2005.

[17]Jonkman, J. and Jonkman, B., NWTC Information Portal, "FAST v8," https://nwtc.nrel.gov/FAST8, 2016–.

[18]Martin, D. P., Johnson, K. E., Zalkind, D. S., and Pao, L. Y., "LPV-Based Torque Control for an Extreme-Scale Morphing Wind Turbine Rotor," Ieee paper, American Control Conference, Seattle, WA, May 2017.

[19]Zalkind, D. S., Pao, L. Y., Martin, D. P., and Johnson, K. E., "Models used for the simulation and control of a segmented, ultralight, morphing rotor," *20th International Federation for Automatic Control (IFAC) World Congress*, Vol. 50, No. 1, 2017, pp. 4478–4483.

[20]International Electrotechnical Commission, I., "IEC 61400-1, Third Ed. 2005-2008. Wind Turbines – Part I: Design Requirements," IEC, 2005.

[21]Noyes, C., Qin, C., and Loth, E., "Ultralight, Morphing Rotors for Extreme-Scale Wind Turbines," AIAA Paper 2017-0924, AIAA Scitech Forum, Grapevine, TX, January 2017.

[22]Yilmaz, O. C., Pires, O., Munduate, X., Sorensen, N., Reichstein, T., Shaffarczyk, A. P., Diakakis, K., Papadakis, G., Daniele, E., Schwarz, M., Lutz, T., and Prieto, R., "Summary of the Blind Test Campaign to Predict the High Reynolds Number Performance of DU00-W-212 Airfoil," *AIAA Paper 2017-0915*, 2017.

[23]AVATAR, "Advanced Aerodynamic Tool for Large Rotors," http://www.eera-avatar.eu, 2017.

[24]Menter, F. R., Langtry, R., and Volker, S., "Transition Modelling for General Purpose CFD Codes," *Flow, Turbulence and Combustion*, Vol. 77, 2006, pp. 277–303.

[25]Bansal, S., Ananda, G. K., and Selig, M. S., "Development of Aerodynamic Analysis Methodology for Segmented Ultralight Morphing Rotors," AIAA Paper 2017-4217, 35th AIAA Applied Aerodynamics Conference, Denver, CO, June 2017.

[26]Ananda, G. K., Bansal, S., and Selig, M., "Subscale Testing of Horizontal-Axis Wind Turbines," AIAA Paper 2017-4216, 35th AIAA Applied Aerodynamics Conference, Denver, CO, June 2017.